



Characterization and kinetics study of poly(α -methyl styrene) synthesized by living anionic polymerization

Mohammadreza Jozaghkar¹ · Farshid Ziaee¹

Received: 26 February 2024 / Accepted: 13 May 2024 / Published online: 24 May 2024
© The Polymer Society, Taipei 2024

Abstract

In this work, poly(α -methyl styrene) (PAMS) was synthesized through living anionic polymerization and characterized by ^{13}C NMR, ^1H NMR, GPC, TGA, DSC. The kinetics study was performed using multi-stage dosing of initiator. The results obtained via GPC analysis revealed that polydispersity index of the synthesized PAMS was close to the true value. Moreover, multi-stage dosing of initiator offers valuable and accurate method to determine propagation rate constant and initial impurities value of the system. ^{13}C NMR analysis demonstrated that Bernoullian statistics model exhibits a superior fit compared to 1st-order Markov statistics model for the assigned sequence. Furthermore, the synthesized PAMS presents higher degree of racemic addition with $P_m=0.439$. ^1H NMR spectroscopy was utilized to ascertain number-average molecular weight of the synthesized samples, corroborating the values estimated through GPC analysis. From the thermal analysis, it was shown that PAMS containing very low molecular weight demonstrates negative glass transition temperature and broad thermal decomposition range.

Keywords Living anionic polymerization · Kinetics study · Poly(α -methyl styrene) · Tacticity · Characterization

Introduction

In the recent years, poly(α -methyl styrene) (PAMS) has captured considerable attention due to its unique chemical structure along with its substantial properties, cost-effectiveness and robust performance in blending modification, adhesive formulation, and paper coating [1, 2]. The synthesis of PAMS involves intricate polymerization processes, with various methods being employed to achieve controlled polymer chain growth [3–5].

Free-radical polymerization of α -methyl styrene, hindered by a low ceiling temperature ($T_c=61\text{ }^\circ\text{C}$), tends to be slow and predominantly yields low molecular weight products due to steric repulsions between substituents in consecutive monomer units [6, 7]. Anionic polymerization is an alternative method which results in well-defined macromolecular structures, providing PAMS with tailor-made properties for specific applications. Employing living polymerization enables precise control over molecular weight and facilitates the addition of co-monomers at any stage of the polymerization

process. This approach yields a diverse array of PAMS homo- and copolymers, thereby expanding the scope of potential applications in various fields [8, 9].

Recently, controlled polymerization of methyl styrene derivatives has been investigated by various researchers. The polymerization of *p*-methyl styrene via controlled cationic polymerization has been carried out by Zhang et al. [10]. They reported that GPC graph of the synthesized sample shows unimodal when ionic liquid was used as reaction medium instead of dichloromethane. Moreover, it was reported that reaction medium has considerable influence on reaction rate and heat release rate. Well-defined poly(methyl styrene-co-styrene) copolymers were synthesized by Wolf et al. [11]. ^{13}C NMR of quaternary aromatic carbon showed diad probabilities and synthetic pathway to favor alternating sequences. The combination of living cationic polymerization and anionic ring-opening polymerizations (AROP) has been used to synthesize linear triblock copolymers containing PAMS, polyisobutylene, and polypivalolactone [12]. Goseki and coworkers suggested oligo (α -methyl styrene) lithium as the initiator for synthesis of 4-halostyrenes via anionic polymerization [13].

Kinetic investigations provide crucial insights into the rate of polymerization, reaction mechanisms, and the

✉ Farshid Ziaee
f.ziaee@ippi.ac.ir

¹ Iran Polymer and Petrochemical Institute, P. O. Box: 14965/115, Tehran, Iran

influence of various parameters on the polymerization process [14, 15]. Understanding these kinetic aspects is pivotal for optimizing reaction conditions, designing tailored polymers, and ensuring reproducibility in the synthesis of PAMS. This includes tailoring molecular weight distribution, end-group functionality, and polymer architecture to meet the desired specifications, thereby advancing the development and application of PAMS in various domains. Moreover, the kinetics study aids in the identification of potential side reactions or undesired processes. It also helps to detect impurity of polymerization system. Our previous research demonstrated the successful calculation of propagation rate constant and amounts of impurities using our novel strategy [16].

To the best of our knowledge, living anionic polymerization of α -methyl styrene along with the investigation of kinetics of polymerization and polymer tacticity have not reported so far. However, delving into the kinetics of PAMS synthesis via living polymerization serves as a foundational pillar for the systematic design and synthesis of polymers endowed with tailored properties and functionalities. Therefore, in this study, living anionic polymerization of α -methyl styrene was conducted and kinetics parameters and impurities amount were estimated using a simple and straightforward method. Moreover, the tacticity, molecular weight, and thermal behavior of the synthesized samples were studied by ^{13}C nuclear magnetic resonance spectroscopy (^{13}C NMR), ^1H nuclear magnetic resonance spectroscopy (^1H NMR), gel permeation chromatography (GPC), thermogravimetric analysis (TGA) and differential scanning calorimetry (DSC), respectively.

Experimental

Materials

All chemicals and reagents including α -methyl styrene monomer (99%), *n*-butyllithium (2.0 M in cyclohexane)

and *sec*-butyllithium (1.4 M in cyclohexane) as initiators, 2-propanol (99.5%) as terminating agent, cyclohexane (99%), concentrated sulfuric acid (98%) and calcium hydride powder (95%) were supplied from Merck, Germany.

Polymerization

The living anionic polymerization of α -methyl styrene unfolded through a meticulous series of steps. All the steps were carried out under Ar atmosphere. Initially, the α -methyl styrene monomer underwent a thorough purification process with calcium hydride powder over a few days to remove dissolved water. Subsequently, the purified α -methyl styrene underwent vacuum distillation at 50 mmHg and 60 °C, streaming into a monomer buret. Meanwhile, cyclohexane was stirred over concentrated sulfuric acid for weeks, followed by inert atmosphere reflux for hours. The pured cyclohexane was then injected into a glass container and transferred to a vacuum glove box. Introducing *n*-butyllithium and monomer into the glass container resulted in a discernible colored solution, confirming successful purification. The solution was then transferred to a polymerization reactor immersed in a thermostated water bath (45 °C \pm 0.1), with purified cyclohexane distilled into the reactor under an Ar atmosphere. The polymerization setup design based on our previous work [16]. For the kinetics study, initiator (*sec*-butyl lithium) addition to the reaction vessel with 200 mL of solvent occurred at specific times via a gastight syringe. Polymerization initiation involved adding purified monomer, and termination, after 4.5 h, utilized degassed 2-propanol. Monomer conversion was assessed using the gravimetric method. Table 1 summarizes the sample designation and composition, maintaining constant initiator amount and polymerization temperature while exploring varied monomer concentrations.

Table 1 Sample designation and compositions for characterization and kinetics study of PAMS synthesized by living anionic polymerization in cyclohexane (200 mL) at 45 °C with initial monomer concentration of 0.15 mol.L⁻¹

Sample name	Peak number	Initiator (mL)	Polymerization time (min)	$M_n (\times 10^3)^a$	$M_n (\times 10^3)^b$	\bar{D}
PAMS I	---	2.5	20	640	730	1.27
PAMS II	---	2.5	270	3800	---	1.09
PAMS III	G1	1	20	18.81	---	1.11
	G2	2	270	3.37	---	1.11
PAMS IV	G1	0.5	80	29.68	---	1.0
	G2	0.5	170	10.25	---	1.01
	G3	0.5	270	5.15	---	1.02

^aMeasured by GPC

^bMeasured by ^1H NMR

Characterization

GPC

GPC analysis was carried out in tetrahydrofuran (THF) at $1 \text{ mL}\cdot\text{min}^{-1}$ and at a temperature of $30 \text{ }^\circ\text{C}$ over Agilent 1100 (USA). The system was outfitted with a differential refractometer detector and a PLgel $5 \text{ }\mu\text{m}$ OH-MIXED C $300 \times 7.5 \text{ mm}$ column, which included an Agilent polystyrene standard, and the concentration of the solution under examination was maintained at 1 g/L .

NMR

The solution NMR analysis was performed using a Bruker Avance 400 MHz instrument (Germany). The sample concentration was around 20% (w/v) for ^{13}C NMR and 5% (w/v) for ^1H NMR, and a 5 mm NMR tube was used at $20 \text{ }^\circ\text{C}$. The ^1H NMR analysis was conducted using 32 K data points, with a spectral width of 16 ppm, an acquisition time of 1.59 s, a relaxation delay of 10 s, a pulse width of 30° , and 4 scans. The ^{13}C NMR spectra were scanned over 64 K data points, with a spectral width of 220 ppm, an acquisition time of 1.59 s, a relaxation delay of 2 s, a pulse width of 90° , and 20,000 scans.

Thermal analysis

TGA analysis was conducted from 25 to $600 \text{ }^\circ\text{C}$ and at a heating rate of $10 \text{ }^\circ\text{C}/\text{min}$ via Toledo instrument (Switzerland). The sample mass was about 2.8 mg. The DSC analysis was performed at the heating rate of $10 \text{ }^\circ\text{C}/\text{min}$ via Toledo

(Switzerland). The sample mass and gas flow rate were about 8 mg and $50 \text{ mL}/\text{min}$ respectively. Aluminum crucible was used for the analysis. Both thermal analyses were carried out under nitrogen atmosphere.

Results and discussion

^{13}C NMR of PAMS

In order to comprehend the architecture of polymer chains, it is imperative to gain insight into the correlation between their structure and characteristics [17]. Primarily, owing to its superior resolution and broader spectral range, ^{13}C NMR spectroscopy is employed for determining the tacticity of polymers [18]. In ^{13}C NMR spectra, each peak can be associated with a distinct sequence characterized by a unique chemical shift. Figure 1 illustrates ^{13}C NMR of PAMS II with narrow D (obtained by GPC, Fig. 2) and with the chemical shifts correspond to various carbon types, including α -methyl carbon, methylene carbon, quaternary aliphatic carbon, quaternary aromatic C1 carbon, and C2, C3, and C4 carbons. These carbon atoms exist within diverse isomeric environments along the polymer chain, leading to mutual influences among neighboring carbon atoms. In this study, the investigation of stereospecificity focused on methylene, quaternary aliphatic, and quaternary aromatic carbons. These assignments are adapted to our previous research [27].

The ^{13}C NMR spectra of quaternary aromatic carbon are depicted in Fig. 3a. The quaternary aromatic carbon within the molecular chain of PAMS exhibits symmetry with varying stereospecificity. Figure 3a illustrates the splitting of

Fig. 1 ^{13}C NMR spectrum of synthesized PAMS via living anionic polymerization

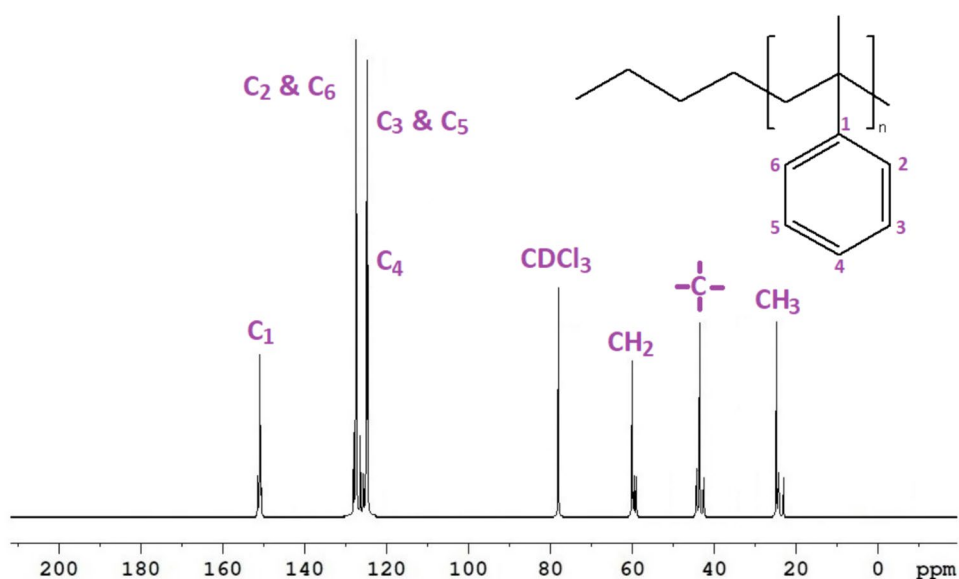
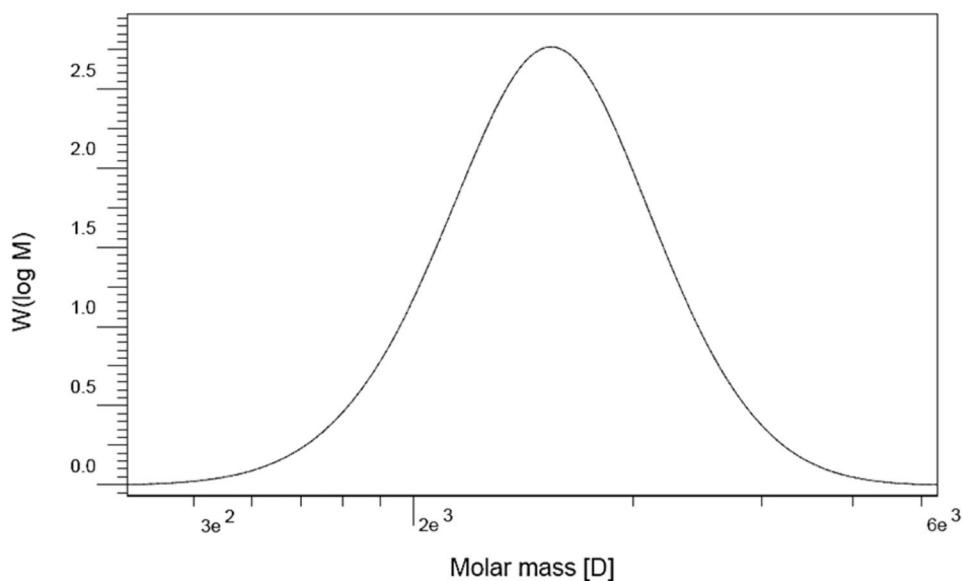


Fig. 2 GPC chromatogram of PAMS II synthesized via living anionic polymerization



the quaternary aromatic carbon into 8 pentad sequences. Hence, in statistical analysis, pentad sequence distributions reveal that the left section is abundant in meso sequences, while the right section is enriched with racemic ones. The upfield region of the quaternary aliphatic carbon of PAMS is enriched with isotactic sequences, whereas the downfield region is abundant in syndiotactic sequences [19]. The distribution of sequences, assignment of chemical shift, experimental peak intensity, and intensities calculated from Bernoullian and 1st-order Markov statistics for the pentad sequences are presented in Table 2. Notably, the measured and calculated values, in accordance with Bernoullian statistics, demonstrate satisfactory agreement. Within the domain of statistical analysis, meso (P_m) and racemic (P_r) sequence probabilities are defined by Eqs. (11) and (12) respectively. The rr , mr , and mm triad sequences denote the syndiotactic, atactic, and isotactic segments of the chain respectively [20].

$$P_m = (2mm + mr)/2 \quad (1)$$

$$P_r = (2rr + mr)/2 \quad (2)$$

The relationship among pentad, triad, and dyad structures (as defined in Eqs. 3–5) facilitate the deduction of meso sequence probabilities from higher sequences [19].

$$mm = mmmm + mmmr + rmmr \quad (3)$$

$$mr = mrrm + mmrr + rrrm + rrrr \quad (4)$$

$$rr = mrrm + mrrr + rrrr \quad (5)$$

By integrating the areas of sequences depicted in Fig. 3 and applying Eqs. 1–5, the calculated value of P_m for all samples is determined to be 0.439. This suggests that the synthesis of PAMS samples exhibits some deviation from the ideal random case ($P_m=0.5$), with the degree of racemic addition consistently surpassing that of meso addition. This

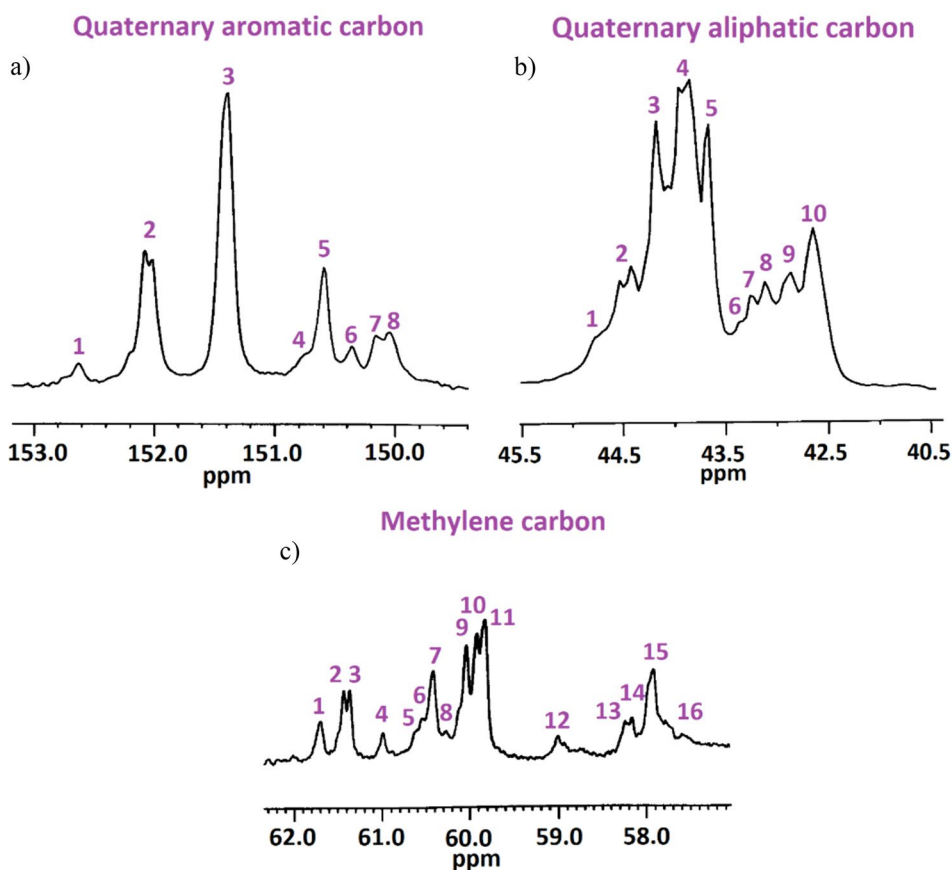
Table 2 Normalized pentad sequences of quaternary aromatic carbon, calculated Bernoullian and 1st-order Markov statistics for PAMS synthesized via living anionic polymerization

Peak No.	Pentad Microstructure	Chemical shift	Obs.	Cal. ^a	Cal. ^b
1	mrrm	152.69	0.0286	0.0375	0.0215
2	mrrr + rrrr	152.12	0.2030	0.4997	0.5546
3	rmrr	151.38	0.4036	0.2071	0.1323
4	mrrm	150.75	0.0257	0.0285	0.1232
5	rmmr	150.58	0.1474	0.0814	0.0584
6	mmrr	150.35	0.0448	0.0795	0.0670
7	rmmr	150.17	0.0389	0.0393	0.0220
8	mmmr + mmmm	150.06	0.0892	0.0270	0.0210

^aBernoullian statistic equation, Average sum square difference: 1.12×10^{-1}

^b1st-order Markov statistic equation, Average sum square difference: 2.09×10^{-1}

Fig. 3 Expanded spectra of **a** quaternary aromatic, **b** quaternary aliphatic and **c** methylene carbons of synthesized PAMS via living anionic polymerization



trend may be attributed to the steric hindrance of pendant groups, which tend to spatially segregate and form racemic sequences. Comparing this result with our findings in the previous work, P_m value of synthesized PAMS via living anionic polymerization is much closer to ideal random case rather than those synthesized via photopolymerization at two different temperatures [19]. However, all polymerization condition suggests $P_m < 0.5$, which represents racemic addition predominates over meso addition in PAMS synthesis.

In line with Bernoullian and 1st-order Markov statistical models, the formation of polymeric chains can be anticipated. For instance, in the 1st-order Markov model, the configuration of the new monomer is influenced by the preceding sequence to which it is added. By evaluating the sum of squared differences between the two models and experimental data, adjustments to the Bernoullian and 1st-order Markov models can be made for all carbon atoms. Table 2 reveals that for all carbons, the Bernoullian statistics model more effectively predicts the formation of monomers in polymer propagation.

Expanded ^{13}C NMR of quaternary aliphatic carbon

The ^{13}C NMR spectrum of quaternary aliphatic carbon is depicted in Fig. 3b. The quaternary aliphatic carbon within PAMS exhibits asymmetry, rendering it prone to monomer insertion along the molecular chains. Additionally, the resonance of this carbon displays unique chemical shifts attributable to the microstructure of PAMS. As depicted in Fig. 3b, the quaternary aliphatic carbon undergoes a splitting into 10 pentad sequences. The upfield portion of the spectrum exhibits an abundance of isotactic sequences, whereas the downfield region predominantly features syndiotactic sequences. The normalized data are presented in Table 3. The comparison between these two statistical models also involved assessing the sum of squared differences between observed and calculated data. These comparative data are additionally presented in Table 3.

Table 3 Normalized pentad sequences of quaternary aliphatic carbon, calculated Bernoullian and 1st -order Markov statistics for PAMS synthesized via living anionic polymerization

Peak No.	Pentad Microstructure	Chemical shift	Obs.	Cal. ^a	Cal. ^b
1	mrrm	44.75	0.0261	0.0369	0.0156
2	mrrr	44.48	0.0979	0.1611	0.1326
3	rrrr	44.39	0.2341	0.2450	0.5977
4	rmrr + mrrm	43.76	0.1366	0.2526	0.0665
5	mmrr + rrrm	43.59	0.1989	0.1435	0.0932
6	rrmmrr	43.46	0.0273	0.0203	0.0152
7	mrmmrr + mrrmmr	43.37	0.0352	0.0278	0.0045
8	rmmrrr	43.13	0.0456	0.0223	0.0175
9	mmmmrr + rmmmmr + mmmrrm	42.72	0.0972	0.0076	0.0336
10	mmmmmm + mmmmmr + rmmmmr	42.61	0.1011	0.0829	0.0236

^aBernoullian statistic equation, Average sum square difference: 2.97×10^{-2}

^b1st -order Markov statistic equation, Average sum square difference: 1.61×10^{-1}

Expanded ¹³C NMR of methylene carbon

In Fig. 3c, the ¹³C NMR spectrum of the methylene carbon, a symmetric carbon, is illustrated. The spectrum reveals a splitting of the methylene carbon into 16 hexad sequences. Table 4 presents the normalized data for these hexad sequences, accompanied by the sum of squared differences between observed and calculated data. Notably, the measured data demonstrates a close agreement with the calculated values derived from Bernoullian statistics.

Table 4 Normalized hexad sequences of the methylene carbon, calculated Bernoullian and 1st -order Markov statistics for PAMS synthesized via living anionic polymerization

Peak No.	Hexad Microstructure	Chemical shift	Obs.	Cal. ^a	Cal. ^b
1	mrrrm	61.75	0.0423	0.0109	0.0265
2	rrmrm	61.49	0.0523	0.0511	0.0098
3	rrmrr	61.35	0.0520	0.0912	0.0107
4	mmmrr	61.07	0.0205	0.0201	0.0752
5	mmrrm	60.62	0.0236	0.0132	0.0119
6	rmmrr	60.57	0.0368	0.0256	0.0398
7	rmmrm	60.39	0.1398	0.0432	0.0615
8	rrrm	60.24	0.1251	0.0985	0.0632
9	rrrrr	60.07	0.0836	0.2379	0.3798
10	mrrrr	59.92	0.1386	0.0675	0.0108
11	mmm	59.83	0.0417	0.0295	0.0161
12	rrm	59.02	0.0123	0.0392	0.0515
13	rmrrm	58.29	0.0553	0.0592	0.0905
14	rmrrr	58.18	0.1239	0.1426	0.077
15	mmrrr	57.91	0.0371	0.0505	0.0624
16	mmrrm	57.61	0.0153	0.0198	0.0133

^aBernoullian statistic equation, Average sum square difference: 4.30×10^{-2}

^b1st -order Markov statistic equation, Average sum square difference: 1.27×10^{-1}

¹H NMR of PAMS

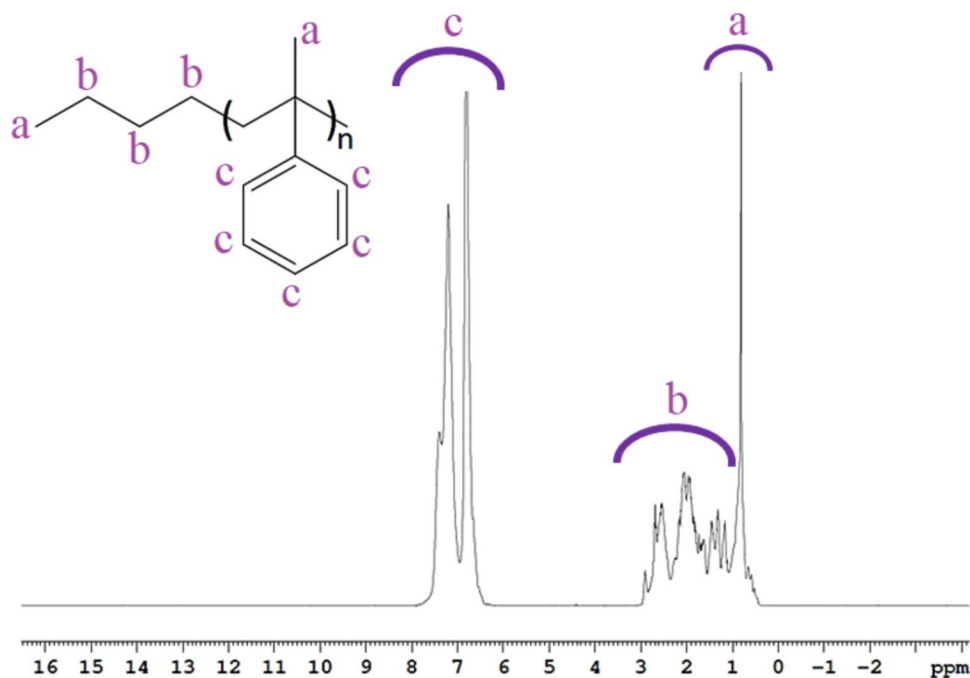
The ¹H NMR spectrum of the synthesized PAMS I is illustrated in Fig. 4. As it can be seen, the peak appeared within the 0.6–1.1 ppm range corresponds to the protons of methyl groups, designated as “a”. Similarly, the peak within the 6.4–7.7 ppm range corresponds to aromatic protons, designated as “c”. Peaks labeled as “b” are ascribed to the protons of aliphatic methine and methylene groups. Notably, the absence of three peaks characteristic of a doublet of doublet within the chemical range of 4–6 ppm confirms the absence of unreacted monomer within the system [16, 21].

Utilizing ¹H NMR as a quantitative methodology offers a straightforward and inherently precise means for determining polymer molecular weights without the need for calibration procedures [22]. M_n of synthesized PAMS I is calculated by assessing the relative intensity of peak of aromatic proton to that of methyl and methylene of repeating unite group [16]. The calculation yields an estimated M_n of 640 gr/mol for the synthesized PAMS I, which closely aligns with the results obtained from GPC analysis. Nonetheless, a minor variance between the results obtained from ¹H NMR and GPC analyses arose from the overlap between CDCl₃ and aromatic proton peaks. It is imperative to emphasize that the accuracy of M_n determination using ¹H NMR spectroscopy is primarily reliable for low molecular weight polymers. This limitation stems from challenges in accurately integrating high molecular weight polymers and the incapacity to detect end groups [16].

Kinetics study

The presence of impurities in living polymerization can considerably impact the end product and properties of the synthesized polymers. Even trace amounts of impurities can disrupt the controlled nature of the polymerization reaction, leading to undesired chain termination or side reactions. This can result in variations in molecular weight, dispersity, and structural

Fig. 4 ^1H NMR spectrum of synthesized PAMS I via living anionic polymerization



defects within the polymer chains. Therefore, meticulous reagent purification assumes paramount importance, given the pivotal role of initiator deactivation contingent upon the absence of impurities such as moisture and oxygen within the system [23, 24]. The impact of these impurities on both molecular weight and the polymerization rate finds elucidation through the scrutiny of GPC distribution plots. Our previous investigation demonstrated the efficiency of utilizing multi-stage initiator dosing for both quantifying the degree of impurity and determining the propagation rate constant (k_p) [16]. Cyclohexane serves as an optimal solvent due to its ability to form stable ion pairs between the active sites and counter ions, thereby enhancing the stability of the anionic system [25]. This methodologically sophisticated approach not only enhances our comprehension of initiator purity implications but also underscores the pivotal role of solvent selection in the intricate dynamics of anionic polymerization, offering valuable insights for advanced polymer engineering in high-impact applications.

Figure 5 illustrates the GPC pattern of PAMS III employing a two-stage dosing strategy. The inset graph highlights the correlation between polymer conversion and the polymerization time. Remarkably, both peaks exhibit polydispersity index (\mathbb{D}) closely aligned with their true values, indicative of a well-controlled polymerization process. As shown in Fig. 5, the peak appeared at higher molecular weight, assigned as “G1”, exhibits a lower intensity compared to peak G2. Furthermore, the recorded conversion rate for step I of dosing was approximately 40%. It is noteworthy that the dissociation of the anionic polymerization initiator before the initiation of the polymerization facilitates the application of simplified classic kinetics for estimation of k_p . Consequently, first-order rate equation was used [26]:

$$[M] = [M]_0 e^{-k_p [I]_0 t} \quad (6)$$

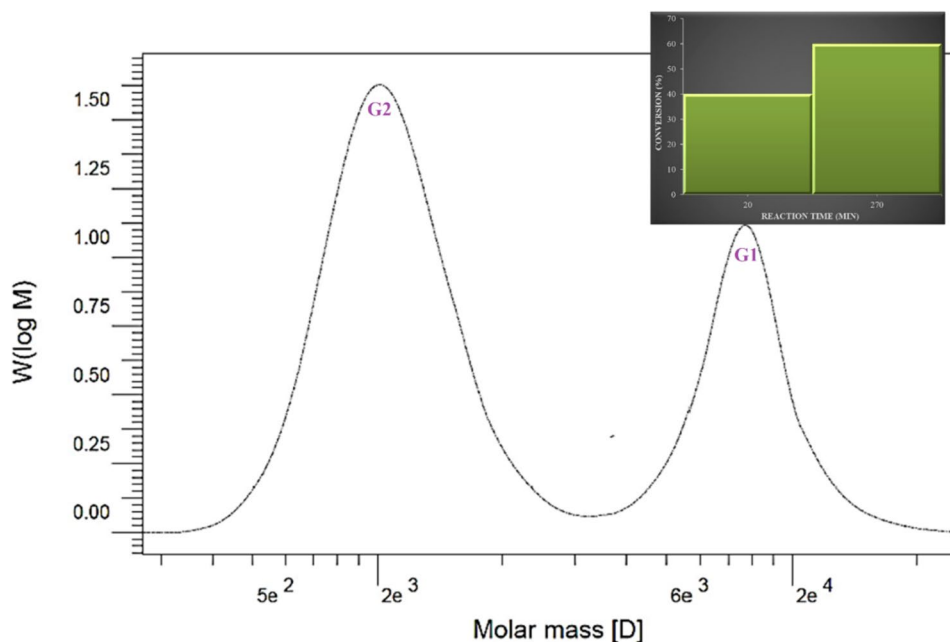
where $[M]$, $[M]_0$ and $[I]_0$ represent the concentration of monomer at time t , the initial concentration of the monomer, and the total concentration of the initiator before dissociation, respectively. $[I]_0$ is the sum of the initial concentration of the pure initiator, $[I]_{0p}$, which could participate in the polymerization reaction, and the primary initiator concentration, $[I]_0$, which reacts with impurities. In order to estimate the $[I]_{0p}$ the degree of polymerization should be defined, which can be obtained from the intensity of each peak in GPC graph. Equations 7 and 8 represent the degree of polymerization for each stage [16].

$$X_{n1} = \frac{[M]_0 - [M]_1}{[I]_{0p}} + \frac{[M]_1 - [M]_2}{[I]_{0p} + [I]_1} \quad (7)$$

$$X_{n2} = \frac{[M]_1 - [M]_2}{[I]_{0p} + [I]_1} = \frac{[M]_1}{[I]_{0p} + [I]_1} \quad (8)$$

where $[M]_1$ and $[M]_2$ represent the residual monomer concentration respectively before the 2nd stage of dosing and at the end of polymerization reaction. X_{n1} and X_{n2} designate the number-average degree of polymerization for peaks G1 and G2, respectively. Moreover, $[I]_1$ is initiator concentration in the 2nd stage of dosing. The terms on the right-hand side of the equations illustrates degree of polymerization for each stage of dosing. Although, gravimetry analysis endorsed the complete monomer conversion, we proceeded to apply another initiator dosing after given time for other samples under similar experimental conditions. The absence of third peak on GPC spectrum corroborated a 100% monomer conversion for this

Fig. 5 GPC chromatogram of PAMS III synthesized via living anionic polymerization (Inset: conversion as a function of polymerization time)



polymerization method. $[I]_{0p}$ could be determined by simultaneously solving Eqs. 7 and 8 and using X_{n1} and X_{n2} values from GPC distribution plot. The obtained parameters were then substituted in the Eq. 1 to attain k_p ($0.51 \text{ L}\cdot\text{mol}^{-1}\cdot\text{sec}^{-1}$).

It is worth noting to mention that by increasing dosing stage, the accuracy of calculated k_p would enhance. Thereupon, PAMS IV synthesized using three-stage dosing of initiator and the corresponding GPC graph is depicted in Fig. 6. The same trend was observed for PAMS IV. Indeed, the peak G1, appeared at higher molecular weight, represents a lower intensity than peaks G2 and G3. This phenomenon suggests the reaction of impurities with initiator at the initial stage of the polymerization [16]. The monomer conversion for this

stage was 27%. In order to determine $[I]_{0p}$ and k_p of PAMS IV, three following equations are defined to represent the degree of polymerization for each stage of polymerization:

$$X_{n1} = \frac{[M]_0 - [M]_1}{[I]_{0p}} + \frac{[M]_1 - [M]_2}{[I]_{0p} + [I]_1} + \frac{[M]_2 - [M]_3}{[I]_{0p} + [I]_1 + [I]_2}$$

$$X_{n2} = \frac{[M]_1 - [M]_2}{[I]_{0p} + [I]_1} + \frac{[M]_2 - [M]_3}{[I]_{0p} + [I]_1 + [I]_2} \quad (9)$$

$$X_{n3} = \frac{[M]_2 - [M]_3}{[I]_{0p} + [I]_1 + [I]_2} = \frac{[M]_2}{[I]_{0p} + [I]_1 + [I]_2} \quad (10)$$

Fig. 6 GPC chromatogram of PAMS IV synthesized via living anionic polymerization (Inset: conversion as a function of polymerization time)

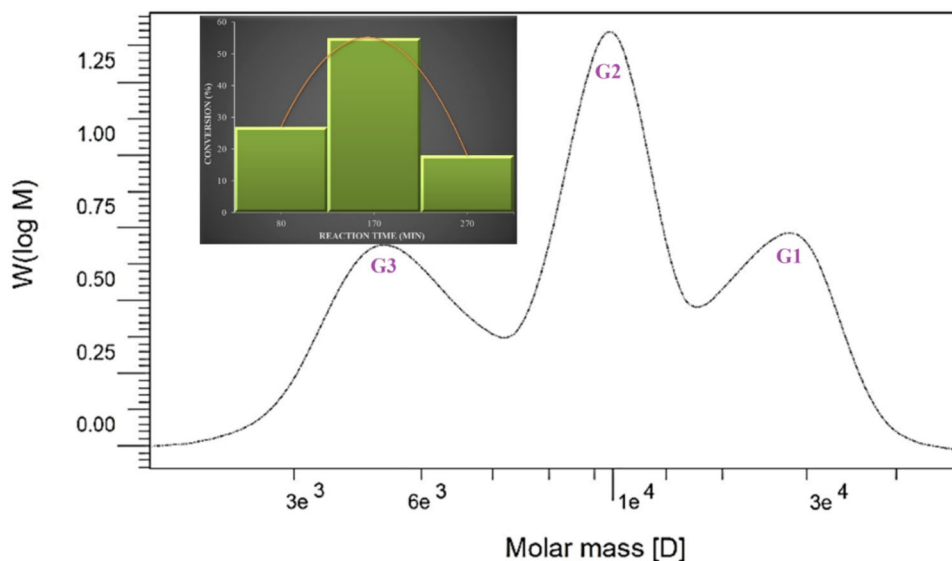
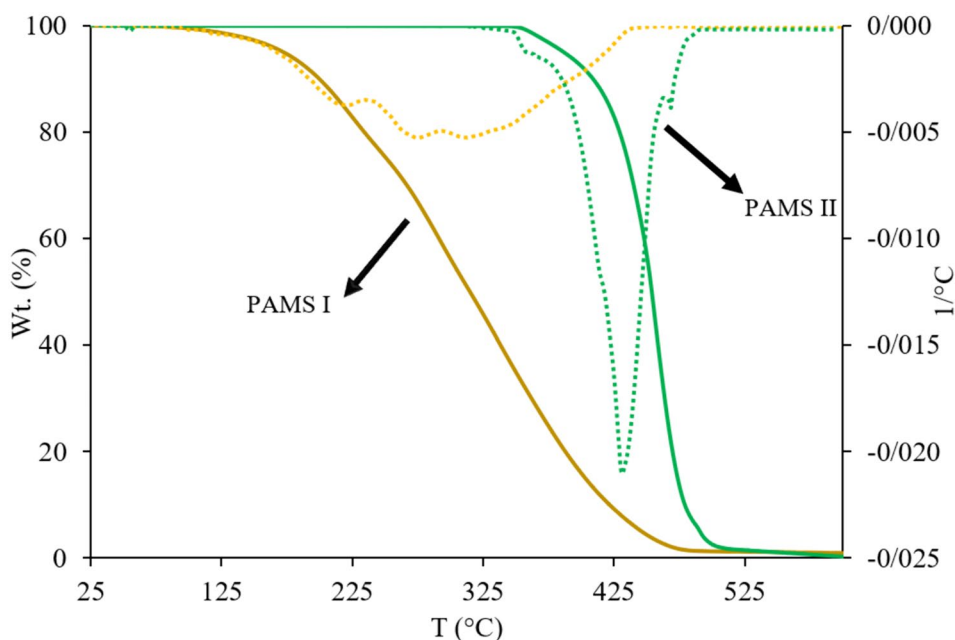


Fig. 7 TGA (solid lines) and DTG (dotted lines) curves for degradation of PAMS I and PAMS II samples



where $[M]_2$ and $[M]_3$ represent the residual monomer concentration respectively before the 3rd stage of dosing and at the end of polymerization reaction. X_{n1} , X_{n2} and X_{n3} designate the number-average degree of polymerization for peaks G1, G2 and G3, respectively. Moreover, $[I]_2$ is initiator concentration in the 3rd stage of dosing. k_p value obtained using three-stage dosing of initiator was $0.49 \text{ L}\cdot\text{mol}^{-1}\cdot\text{sec}^{-1}$, showing well agreement among k_p obtained by two-stage and three-stage dosing. As a matter of fact, the presence of electron donating methyl group in poly(α -methyl styrene) offers lower reaction rate rather than polystyrene synthesized under the same conditions.

Thermal behavior

The physical characteristics of PAMS are significantly influenced by its molecular weight. Figure 7 illustrates the influence of molecular weight on the thermal stability of the synthesized samples. The initial degradation of PAMS I with a molecular weight of 640 g/mol commenced at around 120 °C, while the sample with a higher molecular weight of 3800 g/mol (PAMS II) initiated degradation at approximately 360 °C. A wide and distinct multi-stage degradation pattern is evident in the lower molecular weight resin, indicating a more pronounced influence of the repeating unit [16]. 25% weight loss for each stage suggests depolymerization of the repeating unit in this particular sample. Increasing molecular weight restricts polymer mobility and raises the degradation temperature, implying enhanced thermal stability [27]. The glass transition temperature (T_g) primarily depends on molecular weight, with this influence being particularly significant for polymers characterized by low molecular weights.

The effect on Molecular weight on T_g of PAMS samples is depicted in Fig. 8a. Also, Fig. 8b illustrates DSC curves of PAMS I and PAMS II as an example. As it can be seen from

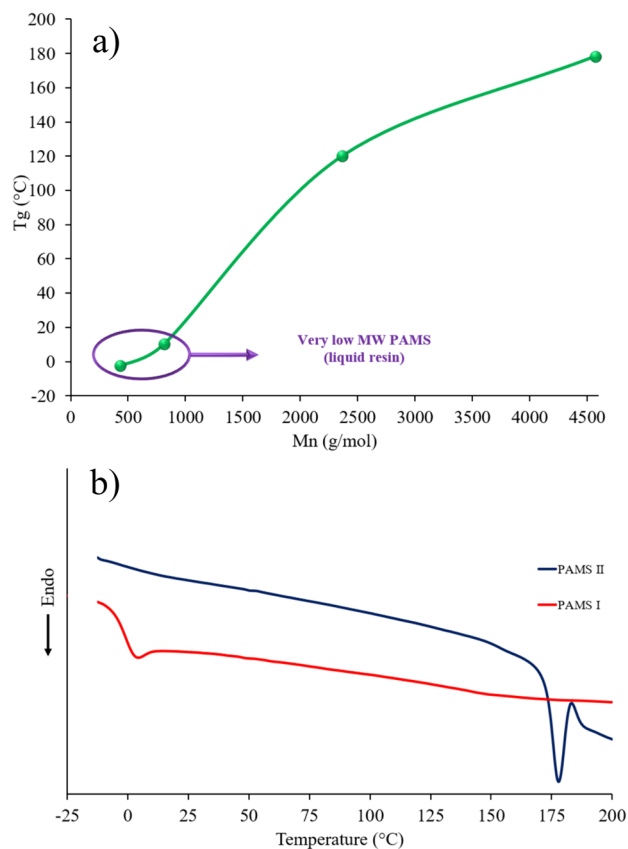


Fig. 8 **a** Plot of T_g versus M_n for PAMS samples with different molecular weight, **b** DSC thermograms for PAMS I and PAMS II

Fig. 8a, a noticeable shift towards higher values of T_g is noted as the molecular weight of PAMS increases. This underscores the correlation between molecular weight and T_g , emphasizing the role of polymerization degree in influencing the glass transition temperature. Illustratively, PAMS I exhibits a sub-zero T_g of $-2.6\text{ }^\circ\text{C}$, whereas PAMS II demonstrates a markedly higher T_g value of approximately $178\text{ }^\circ\text{C}$.

Conclusion

In this study living anionic polymerization of α -methyl styrene was successfully performed and tacticity, microstructure, kinetics, and thermal behavior were investigated. The assignment of all stereosequence was investigated using ^{13}C NMR, which reveals a small deviation from random ideal case with P_m of 0.439. Compared with 1st-order Markov statistics, Bernoullian statistics showed better fit with experimental data. The propagation rate constant and amounts of initial impurities were successfully estimated using multi-stage dosing of initiator along with single GPC pattern. The M_n values derived from quantitative NMR exhibited a remarkable agreement with the results obtained from GPC analysis, underscoring the reliability of quantitative NMR in accurately measuring the M_n of low molecular weight polymers. Thermal behavior represented that very low molecular weight PAMS has broad thermal degradation and negative T_g . These findings not only contribute to the fundamental understanding of controlled polymerization but also open avenues for optimizing reaction conditions and tailoring polymers with enhanced precision.

Data availability The authors declare that data are available whenever are needed.

Declarations

Conflict of interest The authors declare that they have no conflicts of interest.

References

- Pastukhov AV, Pervakov KS, Akunets AA, Kuvshinov IR, Borisenko NG (2022) Fabrication of hollow poly (α -methylstyrene) shells for inertial confinement fusion targets. *J Appl Polym Sci* 139(41):e52997
- Garofalo J, Quinn M, Del Rio E, Benson A, Boehm K (2023) Improving the quality of autonomous inspection for PAMS Mandrels. APS Division of Plasma Physics Meeting Abstracts 2023:CP11-075
- Hu S, Sun W, Fu J, Zhang L, Fan Q, Zhang Z, Tang Y (2017) Reactive molecular dynamics simulations on the thermal decomposition of poly α -methyl styrene. *J Mol Model* 23:1–10
- Halasa AF, Seo KS (2014) Anionic solution copolymerization of α -methylstyrene with conjugated dienes above the ceiling temperature of α -methylstyrene. *Eur Polym J* 51:80–86
- Carvalho MD, Beliido JDA, de Oliveira Siqueira AM, Campos JCC (2020) Stochastic modeling of microstructure of homopolymers and copolymers in batch reactor. *Res Soc Dev* 9(2):e04921930–e04921930
- Banerjee S, Paira TK, Mandal TK (2013) Control of Molecular Weight and Tacticity in Stereospecific Living Cationic Polymerization of α -Methylstyrene at 0 C using FeCl_3 -Based initiators: Effect of Tacticity on Thermal properties. *Macromol Chem Phys* 214(12):1332–1344
- Li Y, Knauss DM (2018) Sequential bulk Anionic polymerization of α -Methylstyrene and isoprene to Form Diblock and Triblock Copolymers. *Macromol Chem Phys* 219(1):1700449
- Higashimura T, Kamigaito M, Kato M, Hasebe T, Sawamoto M (1993) Living cationic polymerization of α -methylstyrene initiated with a vinyl ether-hydrogen chloride adduct in conjunction with tin tetrabromide. *Macromolecules* 26(11):2670–2673
- Xiong Q, Yang S, Peng C, Xie F, Gu Z, Fu Y, Tan H, Dai Q, Yi W, Li L, Liu K (2023) Epoxidation modification of strictly alternating copolymer via living and controlled anionic alternating copolymerization of 1, 3-pentadiene and styrene derivatives. *J Polym Res* 30(8):326
- Zhang X, Tang S, Gao M, Sun C, Wang J (2022) Controlled Cationic polymerization of p-Methylstyrene in Ionic Liquid and its mechanism. *Polymers* 14(15):3165
- Wolf A, Desport JS, Dieden R, Frache G, Weydert M, Poorters L, Schmidt DF, Verge P (2020) Sequence-controlled α -Methylstyrene/Styrene copolymers: syntheses and sequence distribution resolution. *Macromolecules* 53(18):8032–8040
- Wang W, Lu W, Kang NG, Mays J, Hong K (2017) Thermoplastic elastomers based on block, graft, and star copolymers, vol 7. InTech, Rijeka, p 1901679
- Goseki R, Koizumi T, Kurakake R, Uchida S, Ishizone T (2021) Living anionic polymerization of 4-halostyrenes. *Macromolecules* 54(3):1489–1498
- Jozaghkar MR, Ziaee F, Ardakani HR, Ashenagar S, Jalilian M (2019) Kinetics of high-temperature bulk thermal polymerization of methyl styrene. *Iran J Polym Sci Technol* 32:227–240
- Tereshchenko KA, Shiyani DA, Ulitin NV, Kolesov SV, Khursan SL (2022) Experimental study and kinetic modeling of radical-coordination styrene polymerization with participation of ferrocene. *J Polym Res* 29(10):429
- Jozaghkar MR, Ziaee F, Jalilian S (2022) Synthesis, kinetic study and characterization of living anionic polymerized polystyrene in cyclohexane. *Iran Polym J* 31(4):399–412
- Tonelli AE (2017) From NMR Spectra to Molecular Structures and Conformation. *Stereochemistry and Global Connectivity: The Legacy of Ernest L. 2*:161–190
- Ziaee F, Ronagh-Baghbani M, Jozaghkar MR (2020) Microstructure characterization of low molecular weight polybutadiene using the chain end groups by nuclear magnetic resonance spectroscopy. *Polym Bull* 77:2345–2365
- Jozaghkar MR, Ziaee F, Azar AS (2021) Investigation of poly (α -methyl styrene) tacticity synthesized by photo-polymerization. *Polym Bull* 78:5303–5314
- Inoue Y, Nishioka A, Chûjô R (1972) Carbon-13 nuclear magnetic resonance spectroscopy of polystyrene and poly- α -methylstyrene. *Die Makromolekulare Chemie: Macromol Chem Phys* 156(1):207–223
- Osa M, Sumida M, Yoshizaki T, YAMAKAWA H, Ute K, Kitayama T, Hatada K (2000) Determination of Stereochemical compositions of Oligo-and poly (α -methylstyrene) s by ^1H and ^{13}C NMR. *Polym J* 32(4):361–369
- Chen DX, Gao LF, Li XH, Tu YF (2017) Precise molecular weight determination and structure characterization of end-functionalized polymers: an NMR approach via combination of one-dimensional and two-dimensional techniques. *Chin J Polym Sci* 35:681–692
- Ma Q, Leng X, Han L, Liu P, Li C, Zhang S, Lei L, Ma H, Li Y (2020) Regulation of cis and trans microstructures of isoprene units in alternating copolymers via space-limited living species in anionic polymerization. *Polym Chem* 11(15):2708–2714

24. Yang L, Shen H, Han L, Ma H, Li C, Lei L, Zhang S, Liu P, Li Y (2020) Sequence regulation in living anionic terpolymerization of styrene and two categories of 1, 1-diphenylethylene (DPE) derivatives. *Polym Chem* 11(32):5163–5172
25. Hirao A, Hadjichristidis N (2015) Anionic polymerization: principles, practice, strength, consequences and applications. Springer
26. Carraher CE Jr (2017) Introduction to polymer chemistry. CRC Press
27. Mamun A, Rahman SM, Roland S, Mahmood R (2018) Impact of molecular weight on the thermal stability and the miscibility of poly (ϵ -caprolactone)/polystyrene binary blends. *J Polym Environ* 26:3511–3519

Publisher's Note Springer Nature remains neutral with regard to jurisdictional claims in published maps and institutional affiliations.

Springer Nature or its licensor (e.g. a society or other partner) holds exclusive rights to this article under a publishing agreement with the author(s) or other rightsholder(s); author self-archiving of the accepted manuscript version of this article is solely governed by the terms of such publishing agreement and applicable law.